

# Combustion of Energetic Azide Polymers

Naminosuke Kubota\*

Japan Defense Agency, Tachikawa, Tokyo 190, Japan

The combustion-wave structures of azide polymers were examined based on the data obtained by burning-rate and temperature-profile measurements. The energetic azide polymer evaluated in this study was bis-azide methyl oxetan (BAMO), which contains two  $-\text{N}_3$  bonds in the molecular structure. BAMO polymer was copolymerized with tetrahydrofuran and cured with an isocyanate and cross-linked to formulate BAMO copolymer. The results indicate that the burning rate of BAMO copolymer increases with increasing the energy density contained within the unit mass of BAMO copolymer samples. The temperature sensitivity of burning rate is three or four times greater than that of conventional solid propellants. The rate of heat release in the gas phase increases as initial temperature increases at constant pressure. The heat transfer process in the combustion wave is correlated with the observed burning-rate characteristics.

## Nomenclature

$c$	= specific heat, kJ/kgK
$E_s$	= activation energy defined in Eq. (17), kJ/mol
$p$	= pressure, MPa
$Q_d$	= heat of decomposition, kJ/kg
$Q_s$	= heat release at the burning surface, kJ/kg
$q_c$	= rate of heat production, kJ/sm <sup>3</sup>
$q_d$	= conductive heat flux, kJ/sm <sup>2</sup>
$q_s$	= convective heat flux, kJ/sm <sup>2</sup>
$R$	= universal gas constant, $8.314 \times 10^{-3}$ kJ/molK
$r$	= burning rate, m/s
$T$	= temperature, K
$T_a$	= adiabatic flame temperature, K
$t$	= time, s
$x$	= distance, m
$Z_s$	= pre-exponential factor defined in Eq. (17), m/s
$\alpha$	= thermal diffusivity, m <sup>2</sup> /s
$\delta$	= reaction distance, mm
$\lambda$	= thermal conductivity, kW/mK
$\xi$	= $\text{N}_3$ bond density, mol/kg
$\rho$	= density, kg/m <sup>3</sup>
$\sigma_p$	= temperature sensitivity of burning rate defined in Eq. (1), K
$\Phi$	= temperature sensitivity of gas phase defined in Eq. (15), K
$\phi$	= temperature gradient at the burning surface defined in Eq. (10), K/m
$\Psi$	= temperature sensitivity of condensed phase defined in Eq. (16), K
$\psi$	= temperature defined in Eq. (11), K

## Subscripts

$d$	= decomposition
$f$	= final condition
$g$	= gas phase
$p$	= pressure or condensed phase
$s$	= burning surface
$0$	= initial condition

## I. Introduction

**A**ZIDE polymers are unique energetic materials that burn with a very different combustion mode when compared

with nitro compounds such as nitrocellulose and nitroglycerin. Typical azide polymers are glycidyl azide polymer (GAP), bis-azide methyl oxetane (BAMO), and 3-azidemethyl 3'-methyl oxetane (AMMO).<sup>1-3</sup> The  $\text{N}_3$  chemical bonds composing azide polymers release significant heat when they are decomposed thermally. A number of thermochemical studies on azide polymers have been conducted that describe the thermal decomposition chemistry.<sup>4-12</sup>

Since the reaction zone in the condensed phase is a thin and complex structure during burning, very few experimental observations have been done. Brill and his co-workers have conducted a systematic experimental and analytical study in order to determine the effect of mass transfer on fast heating experiments using simultaneous mass and temperature change/Fourier transform infrared (FTIR) spectroscopy.<sup>7-10</sup> They determined the kinetic parameters and found that small molecules are formed by BAMO and GAP, but some large fragments are evolved by AMMO.<sup>8</sup> Since the heat-release process is determined by the kinetics in the reaction zones, the heat transfer process from the high-temperature gas-phase zone to the condensed phase determines the burning rate characteristics. Accordingly, not only thermochemical kinetics, but also heat transfer processes, play important roles in determining the burning-rate characteristics such as pressure and initial-temperature effects.

Extensive experimental and theoretical studies have been done on the combustion wave structures of homogeneous solid propellants, and burning rate models have been proposed in the past to describe the burning-rate characteristics as a function of chemical compositions, pressure, and initial temperature.<sup>13-28</sup> The burning-rate characteristics of this class of propellants are determined by the heat-flux transfer process in the combustion wave. The heat release occurs at the burning surface and in the gas phase just above the burning surface, and temperature increases rapidly in the thin reaction zones.<sup>13-21</sup> Therefore, measurements of the detailed physical and chemical processes of solid propellants are very difficult.

In this study, attention is given to the heat transfer process in the combustion wave of azide polymers that may play a dominant role on the burning-rate characteristics. Burning-rate measurements and temperature-profile measurements in the combustion wave were carried out to obtain information on the effects of energy density of azide polymers, pressure, and initial temperature. An energetic BAMO copolymer was chosen as a typical example of azide polymers.

## II. Formulation of BAMO Copolymer

BAMO polymer has two  $\text{N}_3$  bonds in every BAMO monomer unit. The heat of formation  $\Delta H_f$  of BAMO is a positive

Received Sept. 10, 1994; revision received Dec. 4, 1994; accepted for publication Dec. 19, 1994. Copyright © 1995 by the American Institute of Aeronautics and Astronautics, Inc. All rights reserved.

\*Director, Third Research Center, Technical Research and Development Institute, Sakae 1-2-10. Member AIAA.

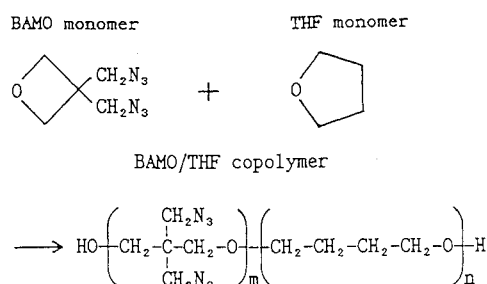


Fig. 1 Synthesis process of BAMO copolymer tested in this study.

value, and the adiabatic flame temperature is higher than that of GAP:

	BAMO polymer	GAP
$\Delta H_f$ at 293 K, kJ/kg	+2460	+957
$T_u$ at 10 MPa, K	2020	1573

In order to formulate BAMO copolymer that was used to measure the burning-rate characteristics and combustion-wave structures, BAMO polymer was copolymerized with tetrahydrofuran (THF).<sup>7</sup> Figure 1 shows the copolymerization process of BAMO polymer with THF. The terminated OH groups of BAMO/THF copolymer was cured with the NCO groups of hexamethylene diisocyanate (HMDI) and cross-linked with trimethylolpropane (TMP).<sup>12</sup> The physiochemical properties of BAMO copolymer used as a reference material in this study are shown as follows:

Chemical formula:	$\text{HO}-(\text{C}_5\text{H}_8\text{N}_6\text{O})_n-(\text{C}_4\text{H}_8\text{O})_m-\text{H}$
Molecular weight:	$2.24 \text{ kg/mol}$ ( $n = 10.4, m = 6.9$ )
Density:	$1.27 \times 10^3 \text{ kg/m}^3$
$\Delta H_f$ at 293 K:	1185 kJ/kg
$T_u$ at 10 MPa:	1524 K

The energy density  $\xi$  of BAMO copolymer is defined as the energy contained within the unit mass of BAMO copolymer. The effect of the energy density on the burning-rate characteristics<sup>8</sup> of BAMO copolymer was determined as a function of  $\xi$ .

### III. Experimental

The experimental investigation on the thermochemical analysis of BAMO copolymer was conducted by differential scanning calorimeter (DSC) to determine the relationship between the burning rate characteristics and energy density of BAMO copolymer. DSC experiments were operated in Ar atmosphere with 167 mm<sup>3</sup>/s flow rate at 0.1 MPa.

The strand-shaped samples (7 mm in diameter and 10 mm in length) of BAMO copolymer were burnt in a chimney-type strand burner<sup>20</sup> that was pressurized with nitrogen. The burning rate and the gas-phase structure were measured with a high-speed video camera through a transparent window attached on the side of the burner. The temperature profiles through the combustion waves were measured by embedding fine thermocouples (Pt-PtRh10%, 5  $\mu\text{m}$  diameter) in the strand samples.<sup>13,18-20</sup> The rate of heat-production and heat transfer process in the combustion waves were determined by the analysis of the  $T$  vs  $t$  data. The methods of manufacture and embedment of these fine thermocouples are described in Ref. 20.

### IV. Results and Discussion

#### A. Energy Density and Burning-Rate Characteristics

Figure 2 shows the results of the heat of decomposition of BAMO copolymer. The relationship between  $Q_d$  and  $\xi$  can be represented by

$$Q_d = 0.6\xi - 2.7$$

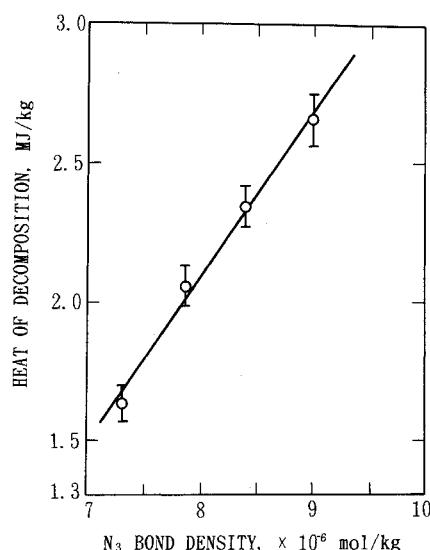


Fig. 2 Heat of decomposition as a function of N<sub>3</sub> bond density within BAMO copolymer.

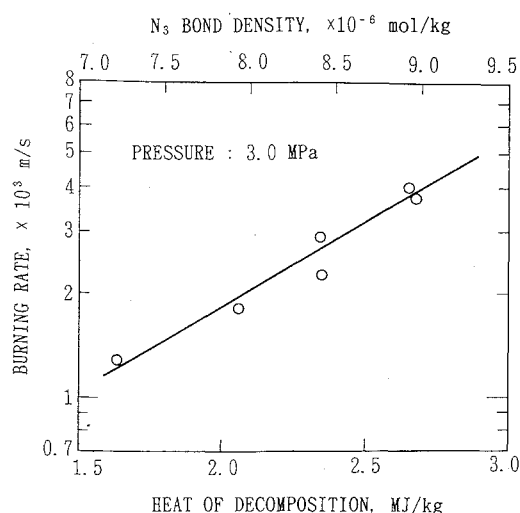


Fig. 3 Burning rate of BAMO copolymer as a function of heat of decomposition and N<sub>3</sub> bond density.

The burning rate ( $T_0 = 293 \text{ K}$ ) of BAMO copolymer composed of different levels of  $\xi$  is shown in Fig. 3 as a function of  $Q_d$ . The linear dependence of the burning rate in this semi-log plot can be given as

$$r = 3.50 \times 10^{-4} \exp(1.10Q_d)$$

The burning rate is also shown in Fig. 4 as a function of pressure and initial temperature. The burning rate increases as pressure increases at constant  $T_0$ , and also increases as initial temperature increases at constant  $p$ , which can be represented by

$$r = 0.55 \times 10^{-3} p^{0.82} \quad \text{at } T_0 = 243 \text{ K}$$

$$r = 2.20 \times 10^{-3} p^{0.61} \quad \text{at } T_0 = 343 \text{ K}$$

The temperature sensitivity of burning rate defined by

$$\sigma_p = \left( \frac{\partial \ln r}{\partial T_0} \right)_p \quad (1)$$

is obtained to be 0.0112/K at  $p = 3.0 \text{ MPa}$ .

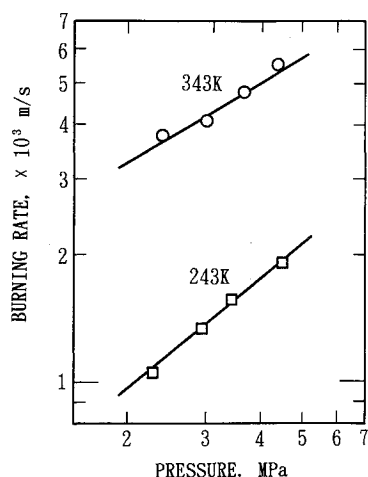


Fig. 4 Burning rate of BAMO copolymer (BAMO/THF = 6/4) as a function of pressure and initial temperature.

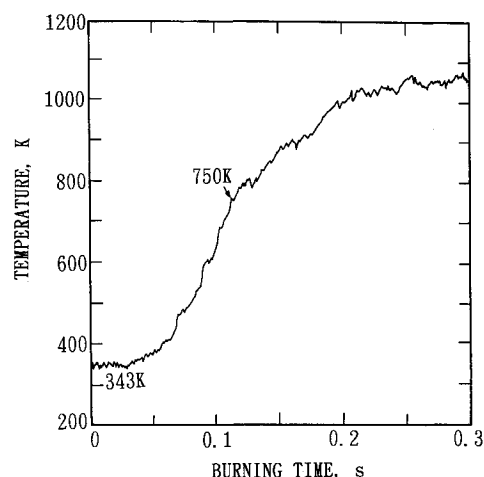


Fig. 6 Temperature profile of BAMO copolymer (BAMO/THF = 6/4) at  $p = 3$  MPa and  $T_0 = 343$  K.

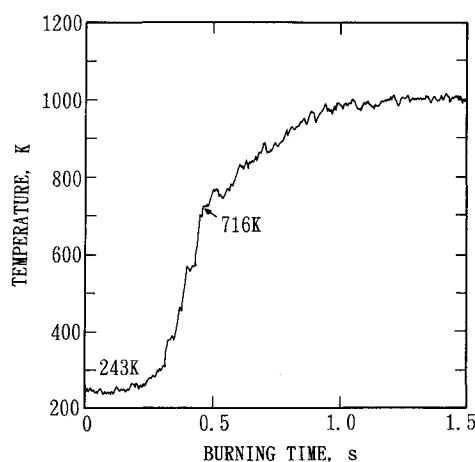


Fig. 5 Temperature profile of BAMO copolymer (BAMO/THF = 6/4) at  $p = 3$  MPa and  $T_0 = 243$  K.

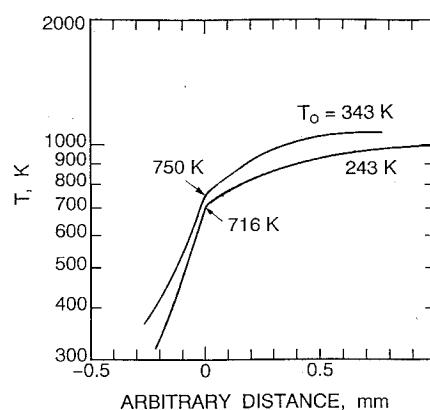


Fig. 7 Determination of  $T_s$  by temperature inflection method from the temperature profile data shown in Figs. 5 and 6.

### B. Combustion-Wave Structure

Typical examples of the temperature profiles in the combustion wave of BAMO copolymer at  $T_0 = 243$  K and  $T_0 = 343$  K are shown in Figs. 5 and 6, respectively. The determination of the burning surface temperature from the temperature profile data was done by the use of "temperature inflection method" described in Ref. 20. The method indicates that temperature increases linearly in a log  $T$  vs  $x$  plot from  $T_0$  to an inflection point where it is determined to be  $T_s$ . As shown in Fig. 7, the  $T_s$  results determined from the data shown in Figs. 5 and 6 are 716 K for  $T_0 = 243$  K and 750 K for  $T_0 = 343$  K, respectively. Figure 8 shows that  $T_s$  increases with increasing  $T_0$ , and  $(\partial T_s / \partial T_0)_p$  is determined to be 0.50 at  $p = 3.0$  MPa.

It is shown from the temperature-profile data that the combustion wave structure consists of several successive zones: nonheated, preheated, surface reaction, gas-phase reaction, and final gas-phase zones. In the nonheated zone, there exists no appreciable thermal effect from the surface, and gas-phase reaction zones and the initial temperature  $T_0$  remains essentially unchanged. In the preheated zone, the temperature increases from  $T_0$  to the burning surface temperature  $T_s$  by heat conduction. At the burning-surface zone, probably including very thin subsurface-reaction zone, decomposition and/or gasification reactions occur.<sup>12</sup> The gaseous and carbonaceous fragments are produced at the burning surface and react exothermically, and temperature increases from  $T_s$  to the combustion temperature  $T_f$  in the gas-phase reaction zone. In the final gas-phase zone, the exothermic reaction terminates and

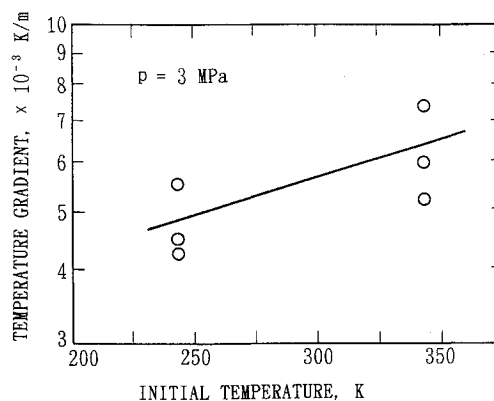


Fig. 8 Temperature gradient in the gas phase at the burning surface of BAMO copolymer (BAMO/THF = 6/4) as a function of initial temperature.

the final combustion products are formed, and temperature reaches the maximum.

In order to investigate the physicochemical process in the subsurface- and surface-reaction zones, an infrared (IR) analysis of a strand-sample that was obtained by combustion interruption was conducted. The interruption was done by a rapid pressure decay of the strand burner from 2 to 0.1 MPa. Figure 9 shows the IR spectra of the nonheated zone and of the surface-reaction zone (0–0.5 mm below burning surface). In the nonheated zone, the absorption of  $N_3$  bond and the absorption of C—O bond, C—H bond, and N—H bond are seen. In the subsurface- and surface-reaction zones, the ab-

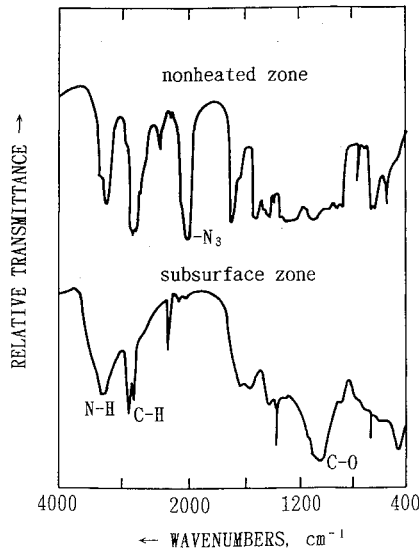


Fig. 9 IR spectra of nonheated and subsurface zones.

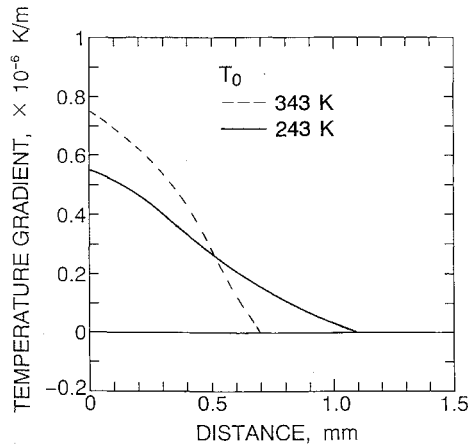


Fig. 10 Temperature gradient in the gas phase ( $p = 3$  MPa) at  $T_0 = 243$  K and 343 K.

sorption of  $N_3$  bond is eliminated. However, the absorption of C—O bond, C—H bond, and N—H bond remains as observed in the nonheated zone. This suggests that an exothermic reaction occurs due to the decomposition of  $N_3$  bonds at the subsurface- and surface-reaction zones. The decomposition process is described in Refs. 8 and 10.

The energy conservation-equation in the gas phase for the steady-state is represented by

$$q_d(x) + q_v(x) + q_c(x) = 0 \quad (2)$$

where

$$q_d(x) = \frac{d}{dx} \left( \lambda_g \frac{dT}{dx} \right) \quad (3)$$

$$q_v(x) = -\frac{mc_g dT}{dx} \quad (4)$$

$$q_c(x) = Q_g \omega_g(x) \quad (5)$$

If one assumes that physical properties of  $\lambda_g$  and  $c_g$  are constant in the gas phase, Eq. (2) can be represented by

$$\lambda_g \frac{d^2 T}{dx^2} - \frac{\rho_p r c_g}{dx} \frac{dT}{dx} + Q_g \omega_g(x) = 0 \quad (6)$$

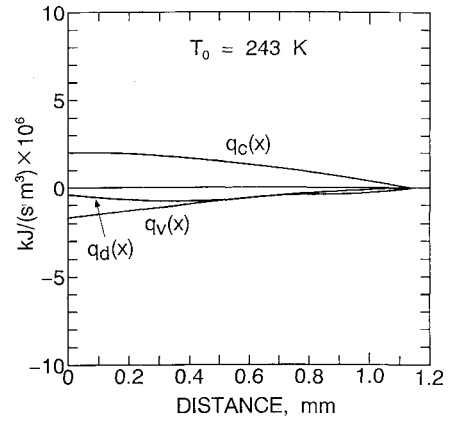


Fig. 11 Heat transfer in the gas phase ( $p = 3$  MPa) at  $T_0 = 243$  K.

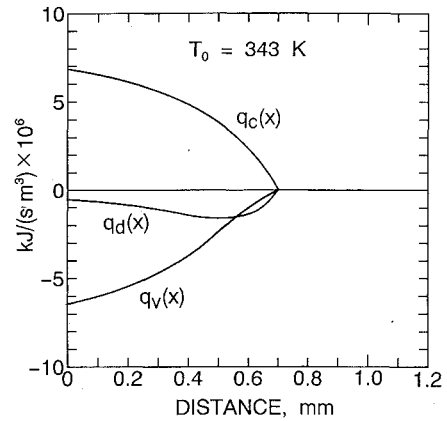


Fig. 12 Heat transfer in the gas phase ( $p = 3$  MPa) at  $T_0 = 343$  K.

where the mass conservation-equation is represented by

$$m = \rho_g u_g = \rho_p r \quad (7)$$

The overall reaction rate in the gas phase  $\bar{\omega}_g$  can be represented by

$$\bar{\omega}_g \delta = \int \omega_g(x) dx = m \quad (8)$$

In order to understand the heat transfer process in the combustion wave of BAMO copolymer, Eq. (6) is adapted to analyze the temperature-profile data shown in Figs. 5 and 6. As shown in Fig. 10, the temperature gradient in the gas-phase reaction zone decreases rapidly as distance increases for both  $T_0 = 243$  K and 343 K. Based on the data shown in Figs. 5 and 6 and using Eq. (6), the conductive heat-flux, convective heat-flux, and the rate of heat release in the gas phase are obtained as shown in Figs. 11 and 12. In the computations of the thermal analysis, the following numerical values are used:  $\rho_p = 1.27 \times 10^3$  kg/m<sup>3</sup>,  $\lambda_g = 1.01 \times 10^{-3}$  kJ/smK,  $c_g = 1.61$  kJ/kgK, and  $r = 1.37 \times 10^{-3}$  m/s at  $T_0 = 243$  K,  $r = 4.20 \times 10^{-3}$  m/s at  $T_0 = 343$  K at 3 MPa. The averaged heat conductivity in the gas phase was determined by the method described in Ref. 11.

The computed results indicate that  $q_c(x)$  is the highest at the burning surface and decreases as the distance increases for both high and low initial temperatures. The  $q_c(x)_s$  at  $T_0 = 343$  K is 3.3 times higher than the  $q_c(x)_s$  at  $T_0 = 243$  K, and the reaction distance in the gas phase is 1.1 mm for  $T_0 = 243$  K and 0.7 mm for  $T_0 = 343$  K. Using the data of Figs. 10 and 11 and Eqs. (7) and (8), the  $\bar{\omega}_g$  is determined to be  $1.58 \times 10^3$  kg/m<sup>3</sup>s at  $T_0 = 243$  K and  $7.62 \times 10^3$  kg/m<sup>3</sup>s at  $T_0 = 343$  K at 3.0 MPa. The results show that the gas-

phase reaction rate is increased 4.8 times by the increase of initial temperature from 243 to 343 K.

### C. Temperature Sensitivity of Burning Rate

Since the combustion process of an energetic material is a chemical reaction phenomenon, the burning rate depends on the thermochemical potential of the material and heat feedback mechanism in the combustion wave. The thermochemical potential is increased by the external heat input given to the material, which is consumed in heating up the temperature of the material. Thus, the burning rate appears as a function of the initial temperature, which is the temperature sensitivity of burning rate defined in Eq. (1). There have been numerous experimental and theoretical studies on the temperature sensitivity of burning rate of solid propellants.<sup>29–35</sup> The mathematical models presented in the past successfully predict the burning rate characteristics.<sup>30–34</sup> However, relatively few studies have been done on  $\sigma_p$  of azide polymers.<sup>11</sup> One reason for this is the lack of a basic understanding of the physicochemical processes of azide-polymer combustion. It has been reported that  $\sigma_p$  of GAP is three or four times higher than that of conventional solid propellants.<sup>11</sup> This is considered to be caused by the difference of the physicochemical properties of the materials. In this study, the heat transfer process in the combustion wave of BAMO copolymer was determined through an analysis of a temperature sensitivity mechanism based on the temperature-profile data in the combustion wave of BAMO copolymer.

The temperature sensitivity of the burning rate defined by Eq. (1) is analyzed by the heat balance equation at the burning surface that is represented by<sup>35</sup>

$$r = \alpha_s \phi / \psi \quad (9)$$

where

$$\phi = \left( \frac{dT}{dx} \right)_{s,g} \quad (10)$$

$$\psi = T_s - T_0 - Q_s / c_p \quad (11)$$

$$\alpha_s = \lambda_g / c_p \rho_p \quad (12)$$

When the logarithmic form of the heat balance equation is differentiated with respect to  $T_0$  at a constant pressure, the following is derived:

$$\sigma_p = \left( \frac{\partial \ln \alpha_s}{\partial T_0} \right)_p + \left( \frac{\partial \ln \phi}{\partial T_0} \right)_p - \left( \frac{\partial \ln \psi}{\partial T_0} \right)_p \quad (13)$$

Since the physical properties of  $\lambda_g$ ,  $c_p$ , and  $\rho_p$  are assumed to be independent of  $T_0$ , Eq. (13) is written as

$$\sigma_p = \Phi + \Psi \quad (14)$$

where

$$\Phi = \left( \frac{\partial \ln \phi}{\partial T_0} \right)_p \quad (15)$$

$$\Psi = - \left( \frac{\partial \ln \psi}{\partial T_0} \right)_p \quad (16)$$

It is shown from Eq. (14) that the temperature sensitivity consists of two parameters,  $\Phi$  and  $\Psi$ :  $\Phi$  is the "temperature sensitivity of gas-phase reaction" that is determined by the gas-phase reaction process, and  $\Psi$  is the "temperature sensitivity of condensed phase" that is determined by the condensed-phase reaction process.

One assumes that the burning rate is given by an Arrhenius-type pyrolysis law at the burning surface as

$$r = Z_s \exp(-E_s/RT_s) \quad (17)$$

Differentiating the logarithmic form of Eq. (17) with respect to  $T_0$  at a constant pressure, one gets the relationship of  $T_s$  and  $T_0$  as

$$\left( \frac{\partial T_s}{\partial T_0} \right)_p = \sigma_p RT_s^2 / E_s \quad (18)$$

Based on the temperature profile data of BAMO copolymer tested in this study, the following numerical values are obtained at pressure 3.0 MPa:

$T_0$ , K	243	343
$T_s$ , K	700	750
$\phi$ , K/m	$5.6 \times 10^5$	$7.4 \times 10^5$
$r$ , m/s	$1.37 \times 10^{-3}$	$4.20 \times 10^{-3}$
$\sigma_p$ , /K		0.0112
$\left( \frac{\partial T_s}{\partial T_0} \right)_p$		0.50

Substituting  $T_0$ ,  $T_s$ ,  $\phi$ , and  $r$  into Eqs. (9–12), the heat release at the burning surface is determined as

$$Q_s = 457 \text{ kJ/kg at } T_0 = 243 \text{ K}$$

$$Q_s = 537 \text{ kJ/kg at } T_0 = 343 \text{ K}$$

Based on  $Q_s$  data at high and low temperatures  $(\partial Q_s / \partial T_0)_p$  is determined to be 0.80 kJ/kgK. Using Eqs. (14–16),  $\Phi$  and  $\Psi$  at  $T_0 = 293$  K are determined to be  $\Phi = 0.00278/\text{K}$  and  $\Psi = 0.00863/\text{K}$ , which shows that  $\Psi$  is approximately 3.1 times greater than  $\Phi$ . This indicates that the temperature sensitivity of the burning rate is dominated by the temperature sensitivity of condensed phase. Furthermore, the  $\sigma_p$  obtained by the analysis of the combustion waves is 0.0114/K, which is approximately equal to the  $\sigma_p$  obtained by the measurements of burning rate. Substituting  $(\partial T_s / \partial T_0)_p$ ,  $\sigma_p$ , and  $T_s$  data into Eq. (18), the activation energy at the burning surface is determined to be  $E_s = 98$  kJ/mol for BAMO copolymer tested in this study. The activation energy and  $(\partial T_s / \partial T_0)_p$  of GAP burning are reported to be 87 kJ/mol and 0.481 at 5 MPa, respectively.<sup>11</sup> It should be noted that the burning rate of GAP is 3.4 times higher than that of BAMO copolymer at the same burning conditions ( $p = 3.0$  MPa and  $T_0 = 293$  K), the thermochemical properties such as  $\sigma_p$ ,  $E_s$ , and  $(\partial T_s / \partial T_0)_p$  appear to be approximately equal for both azide polymers.

## V. Conclusions

The burning rate of BAMO copolymer increases as the energy density increases at constant pressure and initial temperature. The rate of heat release that is distributed in the gas-phase reaction zone increases with increasing initial temperature. The temperature sensitivity of the burning rate of BAMO copolymer is three or four times greater than that of conventional solid propellants, which is characterized by the temperature sensitivities of condensed phase and gas phase. The temperature sensitivity of condensed phase is approximately 3.1 times greater than that of gas phase for BAMO copolymer. Although the burning rate of BAMO copolymer is much lower than that of GAP,  $\sigma_p$ ,  $E_s$ , and  $(\partial T_s / \partial T_0)_p$  are determined to be about the same values for both BAMO copolymer and GAP.

## References

- <sup>1</sup>Miller, R. S., Miller, P. A., Hall, T. N., and Reed, R., Jr., "Energetic Prepolymers for Advanced Navy Cast Cured Propellants and Explosives," Naval Research Reviews, 1981.
- <sup>2</sup>Manser, G. E., and Ross, D. L., "Synthesis of Energetic Polymers," ADA120199, 1982.
- <sup>3</sup>Carpenter, W., U.S. Patent 3,139,609, 1964.
- <sup>4</sup>Farber, M., Harris, S. P., and Srivastava, R. D., "Mass Spectrometric Kinetic Studies on Several Azido Polymers," *Combustion and Flame*, Vol. 55, 1984, pp. 203–211.
- <sup>5</sup>Oyumi, Y., and Brill, T. B., "Thermal Decomposition of Energetic Materials 12. Infrared Spectral and Rapid Thermolysis Studies of Azide-Containing Monomers and Polymers," *Combustion and Flame*, Vol. 65, 1986, pp. 127–135.
- <sup>6</sup>Flanagan, J. E., Frankel, M. B., and Woolery, D. O., "Fundamental Studies of Azide Decomposition and Combustion Mechanisms," Air Force Astronautics Lab., AFAL-TR-87-107, Edwards AFB, CA, Jan. 1988.
- <sup>7</sup>Chen, J. K., and Brill, T. B., "Thermal Decomposition of Energetic Materials 50. Kinetics and Mechanism of Nitrate Ester Polymers at High Heating Rates by SMATCH/FTIR Spectroscopy," *Combustion and Flame*, Vol. 85, 1991, pp. 479–488.
- <sup>8</sup>Chen, J. K., and Brill, T. B., "Thermal Decomposition of Energetic Materials 54. Kinetics and Near-Surface Products of Azide Polymers AMMO, BAMO, and GAP in Simulated Combustion," *Combustion and Flame*, Vol. 87, 1991, pp. 157–168.
- <sup>9</sup>Chen, J. K., and Brill, T. B., "Chemistry and Kinetics of Hydroxyl-Terminated Polybutadiene (HTPB) and Diisocyanate-HTPB Polymers During Slow Decomposition and Combustion-Like Conditions," *Combustion and Flame*, Vol. 87, 1991, pp. 217–232.
- <sup>10</sup>Brill, T. B., Brush, P. J., Patil, D. C., and Chen, J. K., "Chemical Pathways at a Burning Surface," *Twenty-Fourth Symposium (International) on Combustion*, The Combustion Inst., Pittsburgh, PA, 1992, pp. 1907–1914.
- <sup>11</sup>Kubota, N., and Sonobe, Y., "Combustion of GAP Propellants," *Propellants, Explosives, Pyrotechnics*, Vol. 13, 1988, pp. 172–177.
- <sup>12</sup>Miyazaki, T., and Kubota, N., "Energetics of BAMO," *Propellants, Explosives, Pyrotechnics*, Vol. 17, 1992, pp. 5–9.
- <sup>13</sup>Heller, C. A., and Gordon, A. S., "Structure of the Gas Phase Combustion Region of a Solid Double Base Propellant," *Journal of Physical Chemistry*, Vol. 59, 1955, pp. 773–777.
- <sup>14</sup>Rice, R. G., and Ginell, R., "Theory of Burning of Double-Base Rocket Propellants," *Journal of Physical and Colloid Chemistry*, Vol. 54, No. 6, 1950, pp. 885–917.
- <sup>15</sup>Parr, R. G., and Crawford, B. L., "A Physical Theory of Burning of Double-Base Rocket Propellants," *Journal of Physical and Colloid Chemistry*, Vol. 54, No. 6, 1950, pp. 929–954.
- <sup>16</sup>Williams, F. A., "Combustion Theory," 2nd ed., Benjamin Cummings Publishing Co., Inc., 1985, Chap. 7.
- <sup>17</sup>Williams, F. A., "Quasi-Steady Gas-Phase Flame Theory in Unsteady Burning of a Homogeneous Solid Propellant," *AIAA Journal*, Vol. 11, No. 9, 1973, pp. 1128–1130.
- <sup>18</sup>Klein, R., Mentser, M., Von Elbe, G., and Lewis, B., "Determination of the Thermal Structure of a Combustion Wave by Fine Thermocouples," *Journal of Physical and Colloid Chemistry*, Vol. 54, No. 6, 1950, pp. 877–884.
- <sup>19</sup>Sabadell, A. J., Wenograd, J., and Summerfield, M., "Measurement of Temperature Profiles Through Solid Propellant Flames Using Fine Thermocouples," *AIAA Journal*, Vol. 3, No. 9, 1965, pp. 1580–1584.
- <sup>20</sup>Kubota, N., Ohlemiller, T. J., Caveny, L. H., and Summerfield, M., "The Mechanism of Super-Rate Burning of Catalyzed Double Base Propellants," Dept. of Aerospace and Mechanical Sciences, Princeton Univ., Rept. AMS 1087 or AD-763786, Princeton, NJ, March 1973.
- <sup>21</sup>Miller, M. S., "In Search of an Idealized Model of Homogeneous Solid Propellant Combustion," *Combustion and Flame*, Vol. 46, 1982, pp. 51–73.
- <sup>22</sup>Beckstead, M. W., Derr, R. L., and Price, C. F., "The Combustion of Solid Monopropellants and Composite Propellants," *Thirteenth Symposium (International) on Combustion*, The Combustion Inst., Pittsburgh, PA, 1971, pp. 1047–1056.
- <sup>23</sup>Beckstead, M. W., "Model for Double-Base Propellant Combustion," *AIAA Journal*, Vol. 18, No. 8, 1980, pp. 980–985.
- <sup>24</sup>Kubota, N., and Masamoto, T., "Flame Structures and Burning Rate Characteristics of CMDB Propellants," *Sixteenth Symposium (International) on Combustion*, The Combustion Inst., Pittsburgh, PA, 1976, pp. 1201–1209.
- <sup>25</sup>Beckstead, M. W., "A Model for Solid Propellant Combustion," *Eighteenth Symposium (International) on Combustion*, The Combustion Inst., Pittsburgh, PA, 1981, pp. 175–185.
- <sup>26</sup>Kubota, N., "Survey of Rocket Propellants and Their Combustion Characteristics," *Fundamentals of Solid-Propellant Combustion*, edited by K. K. Kuo and M. Summerfield, Vol. 90, Progress in Astronautics and Aeronautics, AIAA, New York, 1984, Chap. 1.
- <sup>27</sup>Lengellé, G., Bizot, A., Duterque, J., and Trubert, J. F., "Steady-State Burning of Homogeneous Propellants," *Fundamentals of Solid-Propellant Combustion*, edited by K. K. Kuo and M. Summerfield, Vol. 90, Progress in Astronautics and Aeronautics, AIAA, New York, 1984, Chap. 7.
- <sup>28</sup>Kubota, N., "Flame Structure of Modern Solid Propellants," *Nonsteady Burning and Combustion Stability of Solid Propellants*, edited by L. DeLuca, E. W. Price, and M. Summerfield, Vol. 143, Progress in Astronautics and Aeronautics, AIAA, Washington, DC, 1992, Chap. 7.
- <sup>29</sup>Cohen, N. S., and Flanagan, D. A., "Mechanisms and Models of Solid-Propellant Burn Rate Temperature Sensitivity: A Review," *AIAA Journal*, Vol. 23, No. 10, pp. 1538–1547.
- <sup>30</sup>Glick, R. L., "Temperature Sensitivity of Solid Propellant Burning Rate," *AIAA Journal*, Vol. 5, No. 3, 1967, pp. 586, 587.
- <sup>31</sup>Blair, D. W., "Initial Temperature and Pressure Effects on Composite Solid Propellant Burning Rates: Comparisons with Theory," *AIAA Journal*, Vol. 8, No. 8, 1970, pp. 1439–1443.
- <sup>32</sup>Coates, R. L., "An Analysis of a Simplified Laminar Flame Theory for Solid Propellant Combustion," *Combustion Science and Technology*, Vol. 4, No. 1, 1971, pp. 1–8.
- <sup>33</sup>Kubota, N., Ohemiller, T. J., Caveny, L. H., and Summerfield, M., "Temperature Sensitivity of Double-Base Propellants," *Proceedings of the 8th JANNAF Combustion Meeting*, CPIA Publ. 220, Vol. I, 1971, pp. 387–402.
- <sup>34</sup>Condon, J. A., Renie, J. P., and Osborn, J. R., "Temperature Sensitivity of Propellant Burning Rates," *Combustion and Flame*, Vol. 30, No. 3, 1977, pp. 267–276.
- <sup>35</sup>Kubota, N., "Temperature Sensitivity of Solid Propellants and Affecting Factors: Experimental Results," *Nonsteady Burning and Combustion Stability of Solid Propellants*, edited by L. DeLuca, E. W. Price, and M. Summerfield, Vol. 143, Progress in Astronautics and Aeronautics, AIAA, Washington, DC, 1992, Chap. 4.